Unprecedented Efficiency Increase in a Ternary Polymer Solar Cell Exhibiting Polymer-Mediated Polymorphism of a Non-Fullerene Acceptor

Qingpei Wan, Liwei Ye, Barry C. Thompson*

Department of Chemistry and Loker Hydrocarbon Research Institute, University of Southern California, Los Angeles, California 90089-1661, United States

ABSTRACT: Polymer solar cells, with the assistance of non-fullerene acceptors (NFAs) and ternary blend strategies, have exceeded 18% power conversion efficiency. However, most NFA-based ternary blends are constructed using the strategies developed for polymer-fullerene systems, and intrinsic properties of these NFAs have been overlooked when designing a ternary organic solar cell. Here, using a new NFA 2,2'-((4,4,9,9-tetrahexyl-4,9-dihydro-s-indaceno[1,2-b:5,6-b'] dithiophene-2,7-diyl) bis(methaneylylidene)) bis(1H-indene-1,3(2H)-dione), referred to IDID, as the third component, we observed the appearance of a polymorph of IDID when it was introduced into a PTQ10: PC₆₁BM binary blend and this ternary blend solar cell showed a significant improvement in efficiency from 3.38% to 6.04%. This relative increase (with respect to the best binary cell) is nearly 80% which is the highest among all the reported organic ternary blends to the best of our knowledge. Specifically, IDID was found to be nucleated by the host polymer donor PTQ10 under the assistance of the processing solvent to form a distinct polymorph, as proven by the grazing incidence X-Ray diffraction (GIXRD), differential scanning calorimetry (DSC), and supported by surface energy measurements. More interestingly, IDID, as a third component in the PTQ10: PC₆₁BM system, was found to outperform the structurally similar NFA IDIC, which only boosted the efficiency from 3.38% to 3.55% in ternary polymer solar cells. This work highlights polymer-mediated polymorphism in NFAs as an important consideration in selection of components for and the optimization of ternary organic solar cells.

Polymer solar cells (PSCs) with bulk heterojunction (BHJ) photoactive layers have received significant attention in recent decades due to their notable strengths for enabling large-area fabrication of flexible solar cells via low-cost solutions coating processes. 1-3,4 Ternary organic solar cells consisting of three components in a single active layer have been identified as a simple and low-cost approach for increasing the power conversion efficiency (PCE) and stability of these devices. 5-7,8 Thanks to the rapid development of non-fullerene acceptors (NFAs) over the last five years, the efficiencies of binary organics solar cells have surpassed 18%.9-13 By combining the ternary strategy with the NFAs, the efficiencies of single junction organic solar cells are approaching the 19% landmark. 14-16 Indeed, the four ternary models developed among fullerene systems, such as cascade charger transfer, 17,18 energy transfer, 19 parallel-like, 20 and the alloy model, 21-25 have been successfully applied to NFA-based organic solar cells. For instance, two NFAs with similar fused backbones have been reported to combine and form an alloy acceptor, which effectively addresses the trade-off between photocurrent and voltage and thus maximizes the performance.26-28

In contrast to fullerene acceptors, NFAs such as ITIC and Y6 lead to crystalline domains in the solid-state films that can crystallize in a variety of polymorphs depending on the processing conditions.^{29,30} Different crystalline phases can result in various structural, optical, and electrical proper-

ties, which potentially can affect device performance. For instance, Pfannmöller et al.³¹ revealed that when the polymer PBDB-T acts to nucleate the NFA ITIC, it leads to the formation of a distinct polymorph under the assistance of DIO additive and thermal annealing. The PBDB-T:ITIC blend with the nucleated ITIC polymorph exhibited an 8.5% PCE whereas the blend without the nucleated polymorph exhibited only a 5.6% PCE. Polymorphism is a critical design parameter for semiconducting properties and even minor changes in crystal packing can result in differentiation of electronic properties by orders of magnitude.^{32-34,29} Despite significant progress in building NFA-based ternary solar cells, in the majority of cases the intrinsic and unique crystalline properties of NFAs such as polymorphism have been ignored.

In this letter, inspired by the design strategy presented by Hou et al ^{35,36}, a new NFA named 2,2'-((4,4,9,9-tetrahexyl-4,9-dihydro-s-indaceno[1,2-b:5,6-b'] dithiophene-2,7-diyl) bis(methaneylylidene)) bis(1H-indene-1,3(2H)-dione) and referred to as IDID (Figure 1), has been designed and synthesized. We observed a significantly enhanced PCE in a ternary PSC based on PTQ10³⁷ :PC₆₁BM upon addition of IDID. Specifically, the relative increase in PCE of this ternary blend was found to be nearly 80% (with respect to the best binary blend) which, to the best of our knowledge, is the highest among all reported ternary blends.^{6,38,39} Importantly, relative to pristine IDID films, we found the formation of a distinct IDID polymorph nucleat-

ed by PTQ10 under the assistance of the processing solvent in the ternary solar cells. Additionally, this PTQ10:IDID:PC₆₁BM ternary blend performs significantly better than the analogous blend with IDIC as a control. These results indicate that polymorphism in NFAs, as dictated by interaction with the host polymer, represents an important aspect that needs to be considered when designing and constructing a ternary polymer solar cell, both in terms of component selection and processing optimization.

PTO10 was selected as the donor in this study because it has been demonstrated as the high efficiency and low-cost polymer donor ³⁷ We adopted PC₆₁BM as the acceptor in the parent binary system and maintained the same polymer:fullerene (1:1.2) ratio for all blends so that the only variable is the third component NFA. The chemical structures of the host donor PTQ10, acceptor PC61BM, and the third component IDID are shown in Figure 1. The synthetic route to the novel IDID is described in the supporting information. Specifically, the precursor IDT-CHO was synthesized according to previous literature 40 and then reacted with 1H-Indene-1,3(2H)-dione under basic conditions to perform the Knoevenagel condensation. The optical and electrochemical characteristics used to determine the HOMO and LUMO energies of IDID are shown in Figure S1 and S2. The HOMO and LUMO energy levels of PTQ10 and PC₆₁BM were adopted from the literature.^{21,37}

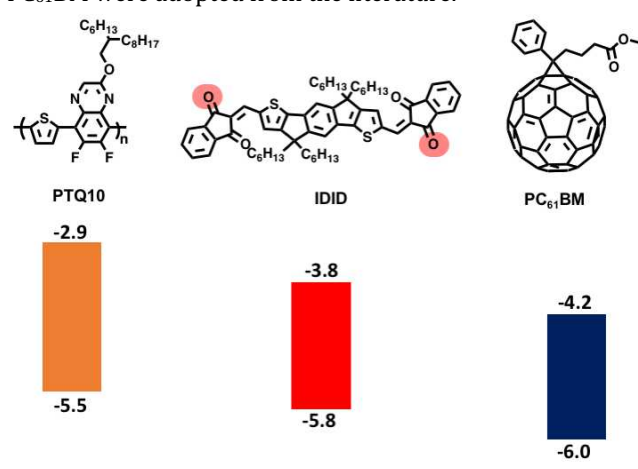


Figure 1. Structures and corresponding HOMO and LUMO energy levels of PTQ10, IDID, and $PC_{61}BM$

Organic solar cells were prepared with the conventional architecture ITO /PEDOT:PSS /PTQ10: NFA: PC61BM /Al. All of the PSCs in this study were processed from o-DCB without post-treatment or additives and were fabricated and measured in air without any encapsulation (average 35% humidity). Binary OSCs made from PTQ10 and PC₆₁BM gave the reasonable PCE of 3.38% (Table 1) with a V_{oc} of 0.858 V, both being similar to literature reports.⁴¹ Ternary devices with a ratio of PTQ10:IDID:PC61BM =1:0.3:1.2 achieved a significantly higher PCE of 6.04%, owing to simultaneous increases in V_{oc} (0.928 V), J_{sc} (11.5 mA/cm²) and fill factor (FF) (57%). Since the fused ring backbone and part of the end group of IDID are identical to the representative NFA IDIC,42 we adopted the use of IDIC as a third component as a control. Interestingly, using IDIC as a third component under the same composition and conditions led to only a slight improvement in efficiency from 3.38% to 3.55% with a J_{sc} of 8.5 mA/cm², V_{oc} of 0.806 V, and a FF of 52%, as shown in Table 1. The introduction

of IDIC didn't significantly increase the efficiency and even led to a lower open circuit voltage. For reference, Welch et al reported a $V_{\rm oc}$ of 0.52V and PCE of 3.4% when fabricating the PTQ10:IDIC binary cells with a conventional architecture and measuring in air.⁴³ In addition, we measured binary blend solar cells of PTQ10:IDID and IDID:PC₆₁BM as controls and the results are shown in Table S2. IDID:PC₆₁BM showed no measurable photovoltaic effect, possibly due to the inability to generate a uniform film. The binary PTQ10:IDID resulted in a PCE of only 0.06%, which might due to the high miscibility of PTQ10 and IDID (*vide infra*).

To contextualize the relative increase in PCE observed upon addition of IDID to the PTQ10:PC $_{61}$ BM binary blend, we compared increases in J $_{sc}$ and PCE between host binary and ternary systems from the literature, 6,38,39 and the results are shown in Figure 2. The relative improvement of J $_{sc}$ is more than 40% and the relative improvement of PCE is close to 80%. Both of these increases are better than all the reported ternary blends in literature, to the best of our knowledge.

Table 1. Photovoltaic Properties of PTQ10:NFA:PC₆₁BM Ternary Blend BHJ Solar Cells at the

mary Brema Brij denar demo at tire				
PTQ10: NFA: PC ₆₁ BM	Jsc	Voc	FF	PCE
	(mA/cm ²	(V)	(%)	(%)
)			
1:0:1.2a	8.0	0.858	49	3.38
1:0.3(IDID):1.2a	11.5	0.928	57	6.04
1:0.3(IDIC):1.2a	8.5	0.806	52	3.55

^a Devices were fabricated with standard conventional architecture ITO/PEDOT:PSS/Active layer/Al, Processed and measured in air without any encapsulations, Posttreatment and additive free, Averages over 7 pixels

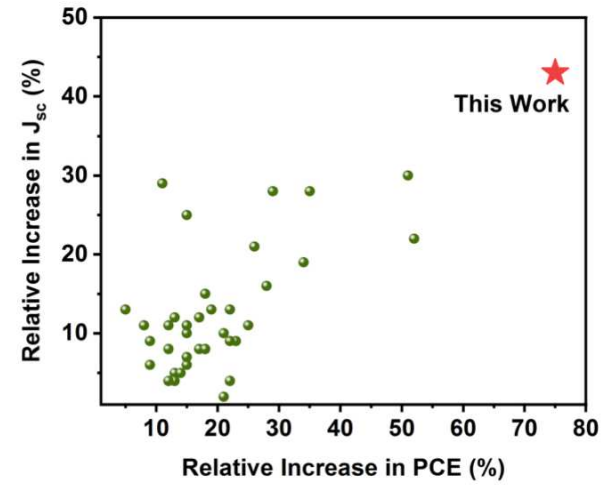


Figure 2. Relative Increase in Jsc and PCE with respect to the best binary cell in literature

To better understand the role of IDID in these ternary solar cells, characterization of the active layer was pursued. Grazing incidence X-ray diffraction (GIXRD) was used to investigate the crystallinity of the different components and blends under processing conditions identical to those used for solar cells active layers with the exception of the neat IDID film which was processed from chloroform since it did not form a film using o-DCB. Neat IDID processed from chloroform with 20 minutes of thermal annealing at 120 °C shows a (100) lamellar peak with 20 of 8.8 degrees, as shown in Figure 3. When IDID was blended with the

donor PTQ10 (1:0.3, w/w) with o-DCB as the processing solvent used for devices under as-cast conditions, the lamellar peak of IDID shifted significantly to 2θ of 9.4 degrees, implying that the molecular packing became more compact after blending with PTQ10 since the d_{100} decreased from 10.0Å to 9.4Å. Additionally, both the stronger peak intensity and the narrower full width at half the maximum (FWHM) indicated an enhanced crystallinity. Crystalline size calculated from the Scherrer equation increased from 7.6nm to 10.7nm for the IDID film and blend film respectively. Thus, we propose that the third component NFA IDID, with the assistance of the processing solvent o-DCB, is likely nucleated by the host donor PTQ10 and forms a distinct polymorph. In order to examine this assumption, we first thermally annealed the PTQ10:IDID blend film (1:0.3, w/w) with the same annealing condition for neat IDID. As a result, the intensity of the IDID lamellar peak clearly decreased, as shown in Figure 3. Correspondingly, the intensity of the PTQ10 lamellar peak increased, as shown in the full GIXRD spectrum (Figures S3 in the Supporting Information). These observations are consistent with evidences used by Bao et al 44,45 to prove the formation of a new polymorph which are typically metastable and require less activation energy to form, whereas the most thermodynamically stable form is the last to appear.^{30,32} The more compact structure of the NFA polymorph in the polymer blend may be due to alignment between the polymer and small molecule due to polymermediated nucleation of the novel polymorph.46

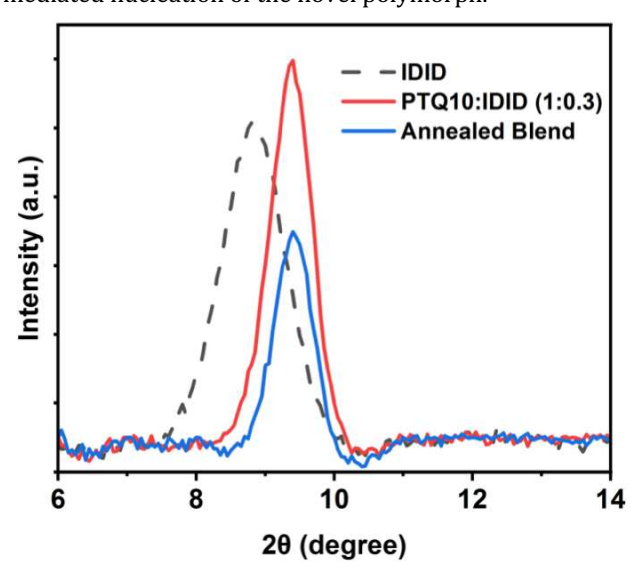
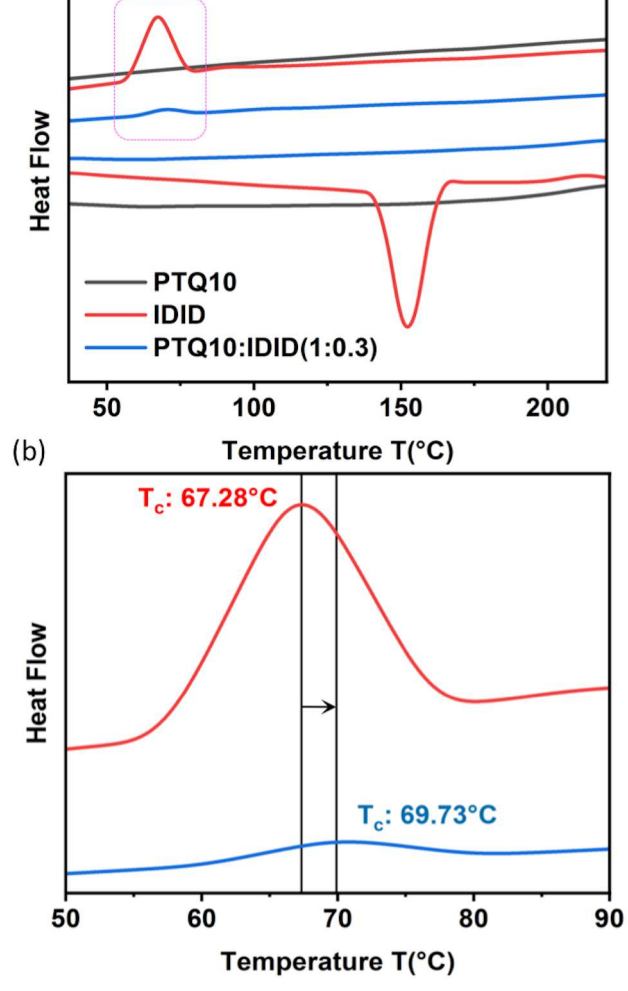


Figure 3. GIXRD patterns of thin film with IDID and the blend with PTQ10 from 2θ =6 to 14 degrees

Interestingly, when we applied the same experiments with IDIC, we did not observe a consequence indicative of any special interaction between IDIC and PTQ10, and the intensity of the peaks of the as-cast NFA were clearly suppressed upon blending with PTQ10 as shown in Figure S4, which matches the observation reported by Li et al. ³⁷ We also studied the PTQ10:IDID blend processed from chloroform for direct comparison to the neat IDID film. The unannealed chloroform blend did not show a lamellar peak for IDID. The lamellar peak for IDID was observed in the blend after annealing (Figure S5), but no peak shift relative to IDID film was observed, indicating the lack of polymorph formation in this case. This observation highlights

the important role of the processing solvent in the formation of the unique polymorph.

In order to further confirm the nucleation between the host polymer donor and the NFA, Differential Scanning Calorimetry (DSC) was employed to evaluate the molecular interaction in all blends. As seen in Figure 4a, PTQ10 did not show any phase transitions during the heating and cooling cycles between 20°C to 220°C, which matches the literature since the melting point of PTQ10 is close to 360°C.47 Considering the melting point of PTO10 is in a range which might cause NFA to decompose, we avoided this melting temperature in our DSC study. The DSC trace of neat IDID showed a sharp melting temperature (T_m) and a crystallization temperature (T_c) of 151.8°C and 67.2 °C, respectively. However, when IDID was blended with PTQ10 with the ratio (1:0.3, w/w) and processed with solvent o-DCB, no endothermic peak was observed during the heating cycle between 20°C to 220°C but there existed a new endothermic peak at 234.9°C as shown in Figure S6, which could correspond to the newly formed polymorph of IDID. Additionally, we observed that the crystallization temperature (Tc) of the blend during the cooling cycle shifted slightly to a higher temperature of 69.7°C, as shown in Figure 4b. This increased crystallization temperature during the cooling cycle has been widely used in polymer blending studies to demonstrate a nucleation effect.⁴⁸ For instance, blending of styrene-ethylene-propylene-styrene (SEPS) triblock copolymer with high-density polyethylene (HDPE) induces a slight shift of Tc for HDPE to a higher value,49 which is similar to the behavior of PTQ10 and IDID reported here. Additionally, after blending with SEPS, the GIXRD peak of HDPE also shifts to a higher angle⁵⁰, which matches our GIXRD observations for PTQ10 and IDID. The nucleation effect of SEPS on HDPE as measured by DSC and GIXRD is analogous to our observations with PTQ10/IDID, which supports the nucleation effect of PTQ10 on IDID to form a distinct polymorph.



(a)

Figure 4. DSC thermograms of (a) PTQ10, IDID, and PTQ10/IDID (1:0.3, w/w) upon heating (down) and cooling (up) with endo down (b) enlarged figure of pink rectangle at the position of $T_{\rm c}$.

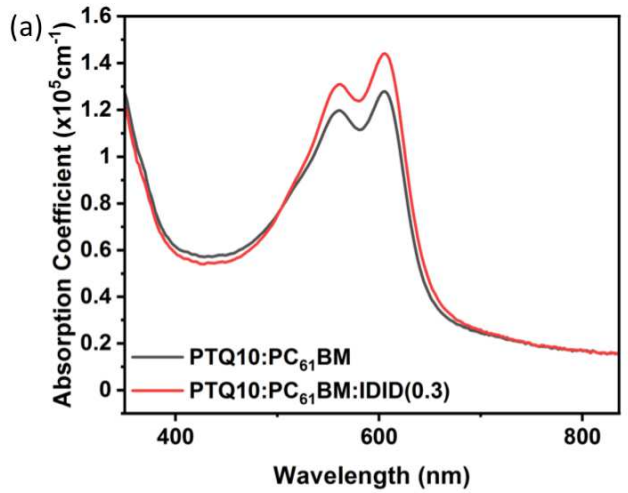
As an additional signature of a nucleation effect, a higher crystallization temperature tail is usually observed, along with an overall shift in the peak towards higher temperature, which is also observed in our study (77.1°C versus 80.0°C, Figure S7). Therefore, we propose that the host donor PTQ10 nucleates IDID to form a distinct polymorph as assisted by processing in *o*-DCB. Since IDIC is the control NFA in this study, we adopted the same DSC analysis for the PTQ10/IDIC blend processed under the same condition as the IDID blend. The results are shown in Figure S8 in the Supporting Information. IDIC has a high melting point, which was observed to decrease after blending with PTQ10. This matches the IDIC melting point depression behavior previously reported. 52

Since the fabricated organic solar cells consist of three components, with the host acceptor $PC_{61}BM$ accounting for roughly half of the active layer, we further investigated whether this nucleation mediated polymorph of IDID does exist in an actual device active layer. First, the GIXRD of the ternary blend $PTQ10:IDID:PC_{61}BM$ (1:0.3:1.2) clearly showed a peak at 20 of 9.4 degrees which is identical to the lamellar peak of the IDID polymorph (20 of 9.4 degrees). Within this region, the control host binary device did not show any peaks (Figures S9 in the Supporting Information).

Second, we measured the surface energy of these compounds based on the two liquid method (Wu model) to investigate the potential interaction between each compound in the ternary blend.⁵³ The surface energy of PTQ10 is 21.4 mN/m with a 107.4° water contact angle and 94.9° glycerol contact angle, which is very close to the value reported by Wantz et al and the water contact angle is nearly the same.41 The surface energy of IDID is 21.7 mN/m with the water contact angle at 101.1° and glycerol contact angle at 90.5°. Since PC61BM has a high surface energy of 27.6 mN/m,⁵⁴ PTQ10 and IDID have a strong possibility of mixing with each other in the ternary blend, which supports our PTQ10:IDID:PC61BM (1:0.3:1.2) ternary GIXRD observations. This further supports that the ternary blend in the device has the unique polymorph caused by the nucleation between PTQ10 and IDID. In contrast, IDIC's surface energy is 25.6 mN/m with the water contact angle at 97.6° and glycerol contact angle at 84.6°. As such, for the IDIC ternary blend, IDIC should preferentially mix with PC₆₁BM because of the relatively close surface energy and this agrees with the reported alloy acceptor formation between fullerene acceptors and NFA acceptors.55

In order to further understand this ternary system and explore the reasons behind the enhanced performance, Ultraviolet-Visible spectroscopy (UV-Vis) have been conducted to compare the PTO10: PC₆₁BM (1:1.2) binary and PTQ10: PC₆₁BM: IDID (1:1.2:0.3) ternary blend. Both binary and ternary films were prepared under the organic solar cell device fabrication conditions, with the thickness about 60nm. As shown in the thin film UV spectroscopy in Figure 5a, the binary PTQ10:PC61BM blend has a slightly higher absorption coefficient before 500nm, which matches the External Quantum Efficiency (EQE) in Figure S10 since the EQE of the binary is higher than the ternary in this region. However, beyond 500nm, the PTQ10:PC₆₁BM:IDID(0.3) ternary blend clearly has a much higher absorption coefficient and the edge slightly shifts to longer wavelength, which might be due to the absorption of IDID itself (in Figure S1). These two factors are also reflected by the EQE in Figure S10. First, the EQE of the ternary blend is obviously higher than the binary blend after 500nm, which could be correlated to the higher absorption coefficient. Second, compared to the binary, the edge of the EQE of the ternary blend is slightly red-shifted as well. As such, the improvement in absorption affected by the addition of IDID can contribute to the enhanced J_{sc} that is observed.

Since the polymer PTQ10 and IDID have similar absorption and the emission of polymer PTQ10 is mainly at 600nm-850nm⁵⁶, we conducted a Photoluminescence(PL) study to compare the binary and ternary blends, as shown in Figure 5b. Interestingly, the photoluminescence (PL) between 600nm and 850nm was further quenched after adding the third component IDID, which suggests improved charger transfer between PTQ10, IDID and PC₆₁BM.^{57,58} Since the surface energy of PTQ10 and IDID are nearly the same, the introduced third component is expected to mainly interact with PTQ10. As we already demonstrated in the manuscript via GIXRD and DSC, IDID is nucleated in the presence of the host donor PTQ10 to form a special polymorph in the ternary blend. Because the polymer PTQ10 is able to induce IDID to form a new polymorph, a special molecular alignment is expected at the interface between the PTQ10 and IDID to promote this nucleation. For instance, Pfannmöller et al.³¹ showed that ITIC formed a new polymorph after thermal annealing because ITIC was able to dock to the polymer PBDB-T and nucleate and grow. Therefore, we infer that the interface between PTQ10 and IDID in the actual ternary blend will be different from the polymer-fullerene interface in the binary blend, and the further quenching in PL is mainly related to this special interface, which will lead to more efficient charge transfer and thus higher J_{sc}. These observations also match what Pfannmöller et al. reported.³¹



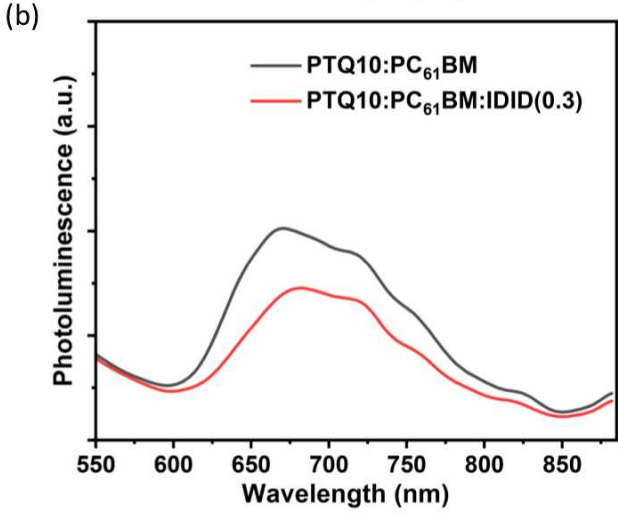


Figure 5. (a) UV-Vis and (b) PL spectra of PTQ10, PC₆₁BM (1:1.2) binary and PTQ10, PC₆₁BM, IDID (1:1.2:0.3) ternary

We have also measured Space-Charge-Limited Current (SCLC) mobility of the binary and ternary blends to further compare the charge transport property. The data overview, hole/electron mobility ratio, and representative *I-V* curve are shown in Figure S12, S13 and Table S4. Adding IDID leads to decreased hole mobility from $9.8 \times 10^{-5} \, cm^2 \, V^{-1} \, S^{-1}$ to 2.7×10^{-5} cm² V⁻¹ S⁻¹ in the ternary blend, which is similar to the result reported by Cho et al. 59 Cho et al. observed the hole mobility was continuously decreasing when introducing the third component NFA IDT2BR into the PPDT2FBT: PCBM binary blend. They ascribed the decreased hole mobility to the presence of IDT2BR in the hole-transporting region. This impact is likely significantly stronger in our case since IDID and PTQ10 have similar surface energy and IDID can be nucleated by the holetransporting polymer PTQ10. Interestingly, we found the electron mobility in our ternary blend was slightly improved from 1.1 × 10⁻⁵ cm² V⁻¹ S⁻¹ to 1.3 × 10⁻⁵ cm² V⁻¹ S⁻¹ while Cho et al. observed a decreased electron mobility and they ascribed it to the low electron mobility of NFA compared with PCBM. We propose the slightly improved electron mobility in our ternary blend is mainly due to the enhanced crystallinity of IDID, which might benefit the charge transport and compensate for its intrinsic low electron mobility.³¹ Importantly, the μ_h/μ_e ratio of the ternary blend (2.0) is significantly better than the binary blend (8.9). This shows that adding the IDID can also balance the charge transport, thus leading to a higher fill factor (FF). Additionally, the open-circuit voltage (Voc) of the ternary blend was increased from 0.86V to 0.93V upon addition of IDID.

In summary, we designed and synthesized a new NFA IDID based on a 1H-Indene-1,3(2H)-dione end group and demonstrated a novel ternary blend where the host polymer donor showed a nucleation effect on IDID and induced IDID to form a new polymorph. Compared with IDIC, IDID has a much lower surface energy and is expected to more strongly interact with the host donor within the ternary blend. GIXRD and the DSC measurements confirmed the unique polymorph of IDID resulting from the o-DCB assisted nucleation between the host donor PTQ10 and third component IDID. More importantly, we observed a close to 80% relative increase in PCE for this ternary blend, which is a new record for PCE improvement when transitioning from a binary to a ternary blend. Importantly, this enhancement is significantly higher than a control with IDIC even though IDIC has been shown to be one of the best performing NFAs and the NFA-fullerene co-acceptor strategy has been widely used for the state-of-the-art. Thus, this work suggests the intrinsic ability of NFAs to form polymorphs must be taken into account when selecting components for ternary blend solar cells and in the optimization of processing conditions.

Supporting Information

General procedures, materials, and characterization methods, spectral mismatch correction, EQE, *J-V* data, GIXRD patterns and data; SCLC hole and electron mobility data. The Supporting Information is available free of charge on the ACS Publications website (PDF).

AUTHOR INFORMATION

Corresponding Author

Barry C. Thompson

Department of Chemistry, Loker Hydrocarbon Research Institute, University of Southern California, Los Angeles, California, 90089-1661, United States

Email: barrycth@usc.edu

ACKNOWLEDGMENT

We acknowledge support by the National Science Foundation (CBET Energy for Sustainability) CBET-1803063. We acknowledge support by the NSF CHE-2018740 for support of X-ray instrumentation. We acknowledge Yunpeng Zhang and Prof. Steve R. Nutt for helping with part of the DSC measurement. We acknowledge Prof. Malancha Gupta for use of the contact angle goniometer.

REFERENCES

- Yu, G.; Gao, J.; Hummelen, J. C.; Wudl, F.; Heeger, A. J. Polymer Photovoltaic Cells: Enhanced Efficiencies via a Network of Internal Donor-Acceptor Heterojunctions. *Science* 1995, 270 (5243), 1789–1791.
- (2) Thompson, B. C.; Fréchet, J. M. J. Polymer–Fullerene Composite Solar Cells. Angew. Chem. Int. Ed. 2008, 47 (1), 58–77.
- (3) Li, G.; Zhu, R.; Yang, Y. Polymer Solar Cells. *Nat. Photonics* **2012**, 6 (3), 153–161.
- (4) Yan, C.; Barlow, S.; Wang, Z.; Yan, H.; Jen, A. K.-Y.; Marder, S. R.; Zhan, X. Non-Fullerene Acceptors for Organic Solar Cells. *Nat. Rev. Mater.* 2018, 3 (3), 18003.
- (5) Ameri, T.; Khoram, P.; Min, J.; Brabec, C. J. Organic Ternary Solar Cells: A Review. Adv. Mater. 2013, 25 (31), 4245–4266.
- (6) Gasparini, N.; Salleo, A.; McCulloch, I.; Baran, D. The Role of the Third Component in Ternary Organic Solar Cells. *Nat. Rev. Mater.* 2019, 4 (4), 229–242.
- (7) An, Q.; Zhang, F.; Zhang, J.; Tang, W.; Deng, Z.; Hu, B. Versatile Ternary Organic Solar Cells: A Critical Review. *Energy Environ. Sci.* 2016, 9 (2), 281–322.
- (8) Xu, X.; Li, Y.; Peng, Q. Ternary Blend Organic Solar Cells: Understanding the Morphology from Recent Progress. Adv. Mater. 2022, 2107476.
- (9) Lin, Y.; Wang, J.; Zhang, Z.-G.; Bai, H.; Li, Y.; Zhu, D.; Zhan, X. An Electron Acceptor Challenging Fullerenes for Efficient Polymer Solar Cells. Adv. Mater. 2015, 27 (7), 1170–1174.
- (10) Zhao, W.; Qian, D.; Zhang, S.; Li, S.; Inganäs, O.; Gao, F.; Hou, J. Fullerene-Free Polymer Solar Cells with over 11% Efficiency and Excellent Thermal Stability. Adv. Mater. 2016, 28 (23), 4734–4739.
- (11) Holliday, S.; Ashraf, R. S.; Wadsworth, A.; Baran, D.; Yousaf, S. A.; Nielsen, C. B.; Tan, C.-H.; Dimitrov, S. D.; Shang, Z.; Gasparini, N.; Alamoudi, M.; Laquai, F.; Brabec, C. J.; Salleo, A.; Durrant, J. R.; McCulloch, I. High-Efficiency and Air-Stable P3HT-Based Polymer Solar Cells with a New Non-Fullerene Acceptor. *Nat. Commun.* 2016, 7 (1), 11585.
- (12) Yuan, J.; Zhang, Y.; Zhou, L.; Zhang, G.; Yip, H.-L.; Lau, T.-K.; Lu, X.; Zhu, C.; Peng, H.; Johnson, P. A.; Leclerc, M.; Cao, Y.; Ulanski, J.; Li, Y.; Zou, Y. Single-Junction Organic Solar Cell with over 15% Efficiency Using Fused-Ring Acceptor with Electron-Deficient Core. *Joule* 2019, 3 (4), 1140–1151
- (13) Li, C.; Zhou, J.; Song, J.; Xu, J.; Zhang, H.; Zhang, X.; Guo, J.; Zhu, L.; Wei, D.; Han, G.; Min, J.; Zhang, Y.; Xie, Z.; Yi, Y.; Yan, H.; Gao, F.; Liu, F.; Sun, Y. Non-Fullerene Acceptors with Branched Side Chains and Improved Molecular Packing to Exceed 18% Efficiency in Organic Solar Cells. Nat. Energy 2021, 6 (6), 605–613.
- (14) Cui, Y.; Xu, Y.; Yao, H.; Bi, P.; Hong, L.; Zhang, J.; Zu, Y.; Zhang, T.; Qin, J.; Ren, J.; Chen, Z.; He, C.; Hao, X.; Wei, Z.; Hou, J. Single-Junction Organic Photovoltaic Cell with 19% Efficiency. Adv. Mater. 2021, 2102420.
- (15) Bi, P.; Zhang, S.; Chen, Z.; Xu, Y.; Cui, Y.; Zhang, T.; Ren, J.; Qin, J.; Hong, L.; Hao, X.; Hou, J. Reduced Non-Radiative Charge Recombination Enables Organic Photovoltaic Cell Approaching 19% Efficiency. *Joule* 2021, 5 (9), 2408–2419.
- (16) Bao, S.; Yang, H.; Fan, H.; Zhang, J.; Wei, Z.; Cui, C.; Li, Y. Volatilizable Solid Additive-Assisted Treatment Enables Organic Solar Cells with Efficiency over 18.8% and Fill Factor Exceeding 80%. Adv. Mater. 2021, 2105301.
- (17) Koppe, M.; Egelhaaf, H.-J.; Dennler, G.; Scharber, M. C.; Brabec, C. J.; Schilinsky, P.; Hoth, C. N. Near IR Sensitization of Organic Bulk Heterojunction Solar Cells: Towards Optimization of the Spectral Response of Organic Solar Cells. Adv. Funct. Mater. 2010, 20 (2), 338–346.
- (18) Ameri, T.; Min, J.; Li, N.; Machui, F.; Baran, D.; Forster, M.; Schottler, K. J.; Dolfen, D.; Scherf, U.; Brabec, C. J. Performance Enhancement of the P3HT/PCBM Solar Cells through NIR Sensitization Using a Small-Bandgap Polymer. Adv. Energy Mater. 2012, 2 (10), 1198–1202.

- (19) Huang, J.-S.; Goh, T.; Li, X.; Sfeir, M. Y.; Bielinski, E. A.; Tomasulo, S.; Lee, M. L.; Hazari, N.; Taylor, A. D. Polymer Bulk Heterojunction Solar Cells Employing Förster Resonance Energy Transfer. *Nat. Photonics* 2013, 7 (6), 479–485.
- (20) Yang, L.; Zhou, H.; Price, S. C.; You, W. Parallel-like Bulk Heterojunction Polymer Solar Cells. J. Am. Chem. Soc. 2012, 134 (12), 5432–5435.
- (21) Khlyabich, P. P.; Burkhart, B.; Thompson, B. C. Compositional Dependence of the Open-Circuit Voltage in Ternary Blend Bulk Heterojunction Solar Cells Based on Two Donor Polymers. J. Am. Chem. Soc. 2012, 134 (22), 9074–9077.
- (22) Khlyabich, P. P.; Burkhart, B.; Thompson, B. C. Efficient Ternary Blend Bulk Heterojunction Solar Cells with Tunable Open-Circuit Voltage. J. Am. Chem. Soc. 2011, 133 (37), 14534–14537.
- (23) Street, R. A.; Davies, D.; Khlyabich, P. P.; Burkhart, B.; Thompson, B. C. Origin of the Tunable Open-Circuit Voltage in Ternary Blend Bulk Heterojunction Organic Solar Cells. J. Am. Chem. Soc. 2013, 135 (3), 986–989.
- (24) Khlyabich, P. P.; Rudenko, A. E.; Thompson, B. C.; Loo, Y.-L. Structural Origins for Tunable Open-Circuit Voltage in Ternary-Blend Organic Solar Cells. Adv. Funct. Mater. 2015, 25 (34), 5557–5563.
- (25) Khlyabich, P. P.; Sezen-Edmonds, M.; Howard, J. B.; Thompson, B. C.; Loo, Y.-L. Formation of Organic Alloys in Ternary-Blend Solar Cells with Two Acceptors Having Energy-Level Offsets Exceeding 0.4 EV. ACS Energy Lett. 2017, 2 (9), 2149–2156.
- (26) Zhan, L.; Li, S.; Lau, T.-K.; Cui, Y.; Lu, X.; Shi, M.; Li, C.-Z.; Li, H.; Hou, J.; Chen, H. Over 17% Efficiency Ternary Organic Solar Cells Enabled by Two Non-Fullerene Acceptors Working in an Alloy-like Model. Energy Environ. Sci. 2020, 13 (2), 635–645.
- (27) Liu, F.; Zhou, L.; Liu, W.; Zhou, Z.; Yue, Q.; Zheng, W.; Sun, R.; Liu, W.; Xu, S.; Fan, H.; Feng, L.; Yi, Y.; Zhang, W.; Zhu, X. Organic Solar Cells with 18% Efficiency Enabled by an Alloy Acceptor: A Two-in-One Strategy. Adv. Mater. 2021, 33 (27), 2100830.
- (28) Fan, B.; Gao, W.; Wang, Y.; Zhong, W.; Lin, F.; Li, W. J.; Huang, F.; Yu, K.-M.; Jen, A. K.-Y. Formation of Vitrified Solid Solution Enables Simultaneously Efficient and Stable Organic Solar Cells. ACS Energy Lett. 2021, 3522–3529.
- (29) Gutierrez-Fernandez, E.; Scaccabarozzi, A. D.; Basu, A.; Solano, E.; Anthopoulos, T. D.; Martín, J. Y6 Organic Thin-Film Transistors with Electron Mobilities of 2.4 Cm ² V ⁻¹ s ⁻¹ via Microstructural Tuning. Adv. Sci. 2021, 2104977.
- (30) Marina, S.; Scaccabarozzi, A. D.; Gutierrez-Fernandez, E.; Solano, E.; Khirbat, A.; Ciammaruchi, L.; Iturrospe, A.; Balzer, A.; Yu, L.; Gabirondo, E.; Monnier, X.; Sardon, H.; Anthopoulos, T. D.; Caironi, M.; Campoy-Quiles, M.; Müller, C.; Cangialosi, D.; Stingelin, N.; Martin, J. Polymorphism in Non-Fullerene Acceptors Based on Indacenodithienothiophene. Adv. Funct. Mater. 2021, 31 (29), 2103784.
- (31) Köntges, W.; Perkhun, P.; Kammerer, J.; Alkarsifi, R.; Würfel, U.; Margeat, O.; Videlot-Ackermann, C.; Simon, J.-J.; Schröder, R. R.; Ackermann, J.; Pfannmöller, M. Visualizing Morphological Principles for Efficient Photocurrent Generation in Organic Non-Fullerene Acceptor Blends. *Energy Environ. Sci.* 2020, 13 (4), 1259–1268.
- (32) Chung, H.; Diao, Y. Polymorphism as an Emerging Design Strategy for High Performance Organic Electronics. *J. Mater. Chem. C* **2016**, *4* (18), 3915–3933.
- (33) Davies, D. W.; Park, S. K.; Kafle, P.; Chung, H.; Yuan, D.; Strzalka, J. W.; Mannsfeld, S. C. B.; Wang, S. G.; Chen, Y.-S.; Gray, D. L.; Zhu, X.; Diao, Y. Radically Tunable N-Type Organic Semiconductor via Polymorph Control. *Chem. Mater.* 2021, 33 (7), 2466–2477.
- (34) Diao, Y.; Lenn, K. M.; Lee, W.-Y.; Blood-Forsythe, M. A.; Xu, J.; Mao, Y.; Kim, Y.; Reinspach, J. A.; Park, S.; Aspuru-Guzik, A.; Xue, G.; Clancy, P.; Bao, Z.; Mannsfeld, S. C. B. Understanding Polymorphism in Organic Semiconductor Thin

- Films through Nanoconfinement. J. Am. Chem. Soc. **2014**, 136 (49), 17046–17057.
- (35) Xian, K.; Cui, Y.; Xu, Y.; Zhang, T.; Hong, L.; Yao, H.; An, C.; Hou, J. Efficient Exciton Dissociation Enabled by the End Group Modification in Non-Fullerene Acceptors. J. Phys. Chem. C 2020, 124 (14), 7691–7698.
- (36) Yang, C.; Zhang, S.; Ren, J.; Gao, M.; Bi, P.; Ye, L.; Hou, J. Molecular Design of a Non-Fullerene Acceptor Enables a P3HT-Based Organic Solar Cell with 9.46% Efficiency. Energy Environ. Sci. 2020, 13 (9), 2864–2869.
- (37) Sun, C.; Pan, F.; Bin, H.; Zhang, J.; Xue, L.; Qiu, B.; Wei, Z.; Zhang, Z.-G.; Li, Y. A Low Cost and High Performance Polymer Donor Material for Polymer Solar Cells. *Nat. Commun.* 2018, 9 (1), 743.
- (38) Huang, H.; Yang, L.; Sharma, B. Recent Advances in Organic Ternary Solar Cells. J. Mater. Chem. A 2017, 5 (23), 11501– 11517.
- (39) Zhang, Y.; Li, G. Functional Third Components in Nonfullerene Acceptor-Based Ternary Organic Solar Cells. Acc. Mater. Res. 2020, 1 (2), 158–171.
- (40) Zhang, W.; Smith, J.; Watkins, S. E.; Gysel, R.; McGehee, M.; Salleo, A.; Kirkpatrick, J.; Ashraf, S.; Anthopoulos, T.; Heeney, M.; McCulloch, I. Indacenodithiophene Semiconducting Polymers for High-Performance, Air-Stable Transistors. J. Am. Chem. Soc. 2010, 132 (33), 11437–11439.
- (41) Szymanski, R.; Henry, R.; Stuard, S.; Vongsaysy, U.; Courtel, S.; Vellutini, L.; Bertrand, M.; Ade, H.; Chambon, S.; Wantz, G. Balanced Charge Transport Optimizes Industry-Relevant Ternary Polymer Solar Cells. Sol. RRL 2020, 4 (11), 2000538.
- (42) Lin, Y.; He, Q.; Zhao, F.; Huo, L.; Mai, J.; Lu, X.; Su, C.-J.; Li, T.; Wang, J.; Zhu, J.; Sun, Y.; Wang, C.; Zhan, X. A Facile Planar Fused-Ring Electron Acceptor for As-Cast Polymer Solar Cells with 8.71% Efficiency. J. Am. Chem. Soc. 2016, 138 (9), 2973–2976.
- (43) Hoff, A.; Farahat, M. E.; Pahlevani, M.; Welch, G. C. Tin Oxide Electron Transport Layers for Air-/Solution-Processed Conventional Organic Solar Cells. ACS Appl. Mater. Interfaces 2022, 14 (1), 1568–1577.
- (44) Yuan, Y.; Giri, G.; Ayzner, A. L.; Zoombelt, A. P.; Mannsfeld, S. C. B.; Chen, J.; Nordlund, D.; Toney, M. F.; Huang, J.; Bao, Z. Ultra-High Mobility Transparent Organic Thin Film Transistors Grown by an off-Centre Spin-Coating Method. *Nat. Commun.* 2014, 5 (1), 3005.
- (45) Chen, J.; Shao, M.; Xiao, K.; He, Z.; Li, D.; Lokitz, B. S.; Hensley, D. K.; Kilbey, S. M.; Anthony, J. E.; Keum, J. K.; Rondinone, A. J.; Lee, W.-Y.; Hong, S.; Bao, Z. Conjugated Polymer-Mediated Polymorphism of a High Performance, Small-Molecule Organic Semiconductor with Tuned Intermolecular Interactions, Enhanced Long-Range Order, and Charge Transport. Chem. Mater. 2013, 25 (21), 4378–4386.
- (46) He, Z.; Zhang, Z.; Bi, S.; Chen, J.; Li, D. Conjugated Polymer Controlled Morphology and Charge Transport of Small-Molecule Organic Semiconductors. Sci. Rep. 2020, 10 (1), 4344
- (47) Peng, Z.; Ye, L.; Ade, H. Understanding, Quantifying, and Controlling the Molecular Ordering of Semiconducting Poly-

- mers: From Novices to Experts and Amorphous to Perfect Crystals. *Mater. Horiz.* **2022**, 10.1039.D0MH00837K.
- (48) Hu, J.; Xin, R.; Hou, C.-Y.; Yan, S.-K.; Liu, J.-C. Direct Comparison of Crystal Nucleation Activity of PCL on Patterned Substrates. *Chin. J. Polym. Sci.* 2019, 37 (7), 693–699.
- (49) Tao, F.; Bonnaud, L.; Murariu, O.; Auhl, D.; Dubois, P.; Bailly, C. A Convenient Route to High-Performance HDPE-CNT Conductive Nanocomposites by Control of Matrix Nucleation. *Macromol. Chem. Phys.* 2012, 213 (21), 2275–2281.
- (50) Yu, X.; Zheng, Z.; Lu, J.; Wang, X. Morphology and Mechanical Properties of Styrene–Ethylene/Butylene–Styrene Triblock Copolymer/High-Density Polyethylene Composites. J. Appl. Polym. Sci. 2008, 107 (2), 726–731.
- (51) Wang, B.; Menyhard, A.; Alfonso, G. C.; Müller, A. J.; Cavallo, D. Differential Scanning Calorimetry Study of Cross-Nucleation between Polymorphs in Isotactic Poly(1-Butene): DSC Study of Cross-Nucleation between Polymorphs in Isotactic Poly(1-Butene). *Polym. Int.* 2019, 68 (2), 257–262.
- (52) Bin, H.; Yang, Y.; Zhang, Z.-G.; Ye, L.; Ghasemi, M.; Chen, S.; Zhang, Y.; Zhang, C.; Sun, C.; Xue, L.; Yang, C.; Ade, H.; Li, Y. 9.73% Efficiency Nonfullerene All Organic Small Molecule Solar Cells with Absorption-Complementary Donor and Acceptor. J. Am. Chem. Soc. 2017, 139 (14), 5085–5094.
- (53) Schmitt, A.; Samal, S.; Thompson, B. C. Tuning the Surface Energies in a Family of Poly-3-Alkylthiophenes Bearing Hydrophilic Side-Chains Synthesized via Direct Arylation Polymerization (DArP). Polym. Chem. 2021, 12 (19), 2840– 2847.
- (54) Khlyabich, P. P.; Rudenko, A. E.; Burkhart, B.; Thompson, B. C. Contrasting Performance of Donor–Acceptor Copolymer Pairs in Ternary Blend Solar Cells and Two-Acceptor Copolymers in Binary Blend Solar Cells. ACS Appl. Mater. Interfaces 2015, 7 (4), 2322–2330.
- (55) Zhao, Q.; Xiao, Z.; Qu, J.; Liu, L.; Richter, H.; Chen, W.; Han, L.; Wang, M.; Zheng, J.; Xie, Z.; Ding, L.; He, F. Elevated Stability and Efficiency of Solar Cells via Ordered Alloy Co-Acceptors. ACS Energy Lett. 2019, 4 (5), 1106–1114.
- (56) Cha, H.; Zheng, Y.; Dong, Y.; Lee, H. H.; Wu, J.; Bristow, H.; Zhang, J.; Lee, H. K. H.; Tsoi, W. C.; Bakulin, A. A.; McCulloch, I.; Durrant, J. R. Exciton and Charge Carrier Dynamics in Highly Crystalline PTQ10:IDIC Organic Solar Cells. Adv. Energy Mater. 2020, 10 (38), 2001149.
- (57) Xie, Y.; Yang, F.; Li, Y.; Uddin, M. A.; Bi, P.; Fan, B.; Cai, Y.; Hao, X.; Woo, H. Y.; Li, W.; Liu, F.; Sun, Y. Morphology Control Enables Efficient Ternary Organic Solar Cells. Adv. Mater. 2018, 30 (38), 1803045.
- (58) Ke, L.; Min, J.; Adam, M.; Gasparini, N.; Hou, Y.; Perea, J. D.; Chen, W.; Zhang, H.; Fladischer, S.; Sale, A.-C.; Spiecker, E.; Tykwinski, R. R.; Brabec, C. J.; Ameri, T. A Series of Pyrene-Substituted Silicon Phthalocyanines as Near-IR Sensitizers in Organic Ternary Solar Cells. Adv. Energy Mater. 2016, 6 (7), 1502355.
- (59) Kim, M.; Lee, J.; Sin, D. H.; Lee, H.; Woo, H. Y.; Cho, K. Nonfullerene/Fullerene Acceptor Blend with a Tunable Energy State for High-Performance Ternary Organic Solar Cells. ACS Appl. Mater. Interfaces 2018, 10 (30), 25570–25579.

